UCRL-JC-131875
Preprint

Development of Ytterbium Doped $Sr_5(PO_4)_3F$ for the Mercury Laser Project

A. Bayramian, C. Bibeau, K. Schaffers, J. Lawson,
C. Marshall, S. Payne, R. Morris

This paper was prepared for submittal to
Fourteenth Topical Meeting on Advanced Solid-State Lasers
Boston, MA
Jan. 31-Feb.3, 1999

January 27, 1999

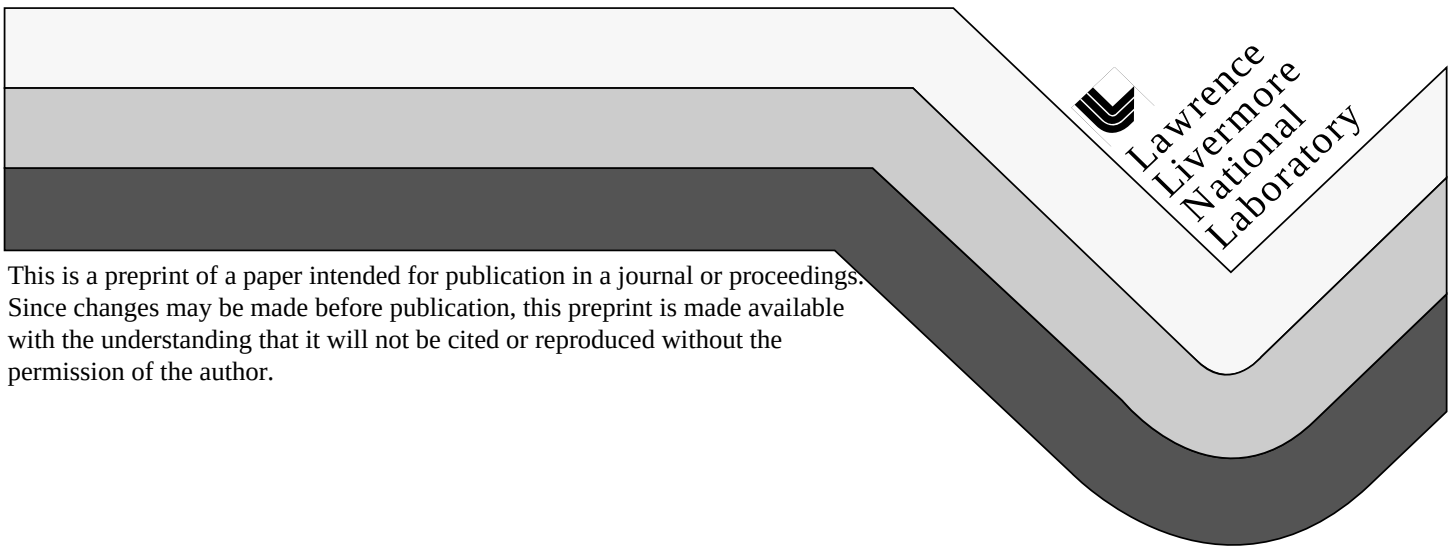

Development of ytterbium doped $Sr_5(PO_4)_3F$ for the Mercury Laser Project

Andy Bayramian, Camille Bibeau, Kathleen Schaffers, Janice Lawson, Chris Marshall, and Stephen Payne

Lawrence Livermore National Laboratory, 7000 East Ave., L-482, Livermore, CA 94551
bayramian1@llnl.gov

Robert Morris

208 Emmans Rd., Flanders, NJ 07836

Abstract: Recent developments in crystal growth, including bulk homogeneity and interferometry, as well as experimental measurement and modeling of the gain saturation of Yb^{3+}:$Sr_5(PO_4)_3F$ are covered.
OCIS codes: (140.3280) Laser amplifiers; (120.5050) Phase measurement; (999.9999) Crystal growth

Introduction

Ytterbium doped $Sr_5(PO_4)_3F$ (S-FAP) has been shown to be a robust laser material ideal for medium power applications such as diode-pumped solid-state laser oscillator[1] and amplifier[2] systems. Currently ytterbium doped S-FAP is being considered for the gain medium in a diode-pumped laser for advanced fusion driver. The first phase of this project, entitled the Mercury Laser, is to build a diode-pumped 100 J, 10 Hz laser system able to operate with temporal pulselengths of 2 to 10 nanoseconds with a 10 % wallplug efficiency. To accomplish this task, 4 x 6 x 0.75 cm slabs of S-FAP are required. Crystals of Yb:S-FAP, grown by using the Czochralski (CZ) method, have been hampered by optical defects such as cracking, cloudiness, bubble core, and grain boundaries which are detrimental to energy extraction. Recent improvements in the growth process have significantly decreased optical defect sites. To quantify improvement in crystal growth, the optical homogeneity has been probed using interferometry. The spatial frequency spectrum can be extracted from the interferograms in the form of Power Spectral Density (PSD) plots which show lower distortion in recent growth runs. In a laser fusion driver, where short, high-fluence pulses will extract the stored energy, gain saturation will also affect the energy extraction. Gain saturation is a measure of the saturation fluence (F_{sat}) of S-FAP which depends inversely on the gain cross section (σ) at the laser frequency (ν) and can be written as $F_{sat} = (h \nu / \sigma) k[g_u, g_L, F_{out}, \tau]$ where k is a dimensionless number representing the deviation from pure two-level homogeneous extraction, and can be a function of the degeneracies of the upper and lower laser levels (g_u and g_L), the output fluence (F_{out}), and the laser temporal pulsewidth (τ)[3].

Crystal Growth

Improvement in the crystal quality of CZ grown Yb:S-FAP has been attributed to a better understanding of the defects (cracking, cloudiness, bubble core, and grain boundaries) and refinement of growth conditions[4]. Cracking has been attributed to large thermal gradients and strain from defect sites in the crystals. Cloudiness in the crystals is caused by second phase precipitation from unstable growth conditions such as fluctuations at the growth interface and variations in melt composition due to the evaporation of SrF_2 at the melt surface. Methods of maintaining a stable melt composition are being

engineered to compensate for evaporation induced composition changes during growth. The boules also experience a post-growth annealing process over the melt which further reduces cloudiness. Bubble core has been traced to constitutional supercooling, which is caused by instability at the growth interface leading to trapped pockets of low melting temperature liquid. Stabilization of the growth interface through controlling thermal gradients, power fluctuations, and composition changes have greatly reduced the bubble core defects. The final issue is the formation of low-angle grain boundaries which are planar groups of dislocations that separate neighboring grains with crystallographic misorientation of $< 5°$ and are visible to the naked eye as refractive index striations through the crystal. These boundaries can be nucleated from the above defects as well as by propagation from the seed to the crystal. Table I summarizes the defects which were characterized, the proposed solutions and the outcome of growth trials using these new techniques. By implementing more stable growth conditions, we have been able to produce Yb:S-FAP crystals with sufficient optical quality to meet the Mercury laser specifications.

Table I. Yb:S-FAP defects and their respective solutions.

Issues	Solution approach	Outcome
✓ Cracking	– Reduce thermal gradients	→ Crack-free large-diameter crystals (≤ 5 cm)
✓ Cloudiness	– Add excess SrF_2 – Post-annealing	→ Clear crystals
✓ Bubble Core	– Maintain constant composition melt – Stabilize growth interface	→ Number of core defects reduced → Limited to central region
~ Grain boundaries	– Use defect-free seeds – Seed extension	→ Crystals have been grown with < 2 grain boundaries

Bulk Homogeneity Measurement

Progress in bulk homogeneity has been monitored by mapping the transmitted phase of several Yb:S-FAP crystals using an interferometer. The phase maps of the homogeneity are converted to Power Spectral Density (PSD) plots, which are the square of the Fourier amplitude spectrum divided by the width of the frequency intervals. The maximum tolerable PSD in any frequency interval is defined by the desired beam characteristics at the output of the laser system and affects the diffraction limited spot size possible with a given beam. Phase maps have confirmed our theory that a core of higher index occurs at the center of the boule due to slightly higher ytterbium concentration, as well as showing that grain boundaries or any imperfection visible to the naked eye have an undesirable affect on the transmitted wavefront. Fig. 1 displays the phase map of a slice from the best Yb:S-FAP boule to date. To achieve the phase plot in Fig. 1, the phase front of the slice had to be subapertured to eliminate the core of the boule. The two dimensional PSD plot of the phase map in Fig. 1 was then integrated according to Eq. 1 to give the 1-D PSD plot in Fig. 2.

$$\mathrm{PSD}(\nu_x) = \int \mathrm{PSD}(\nu_x, \nu_y) d\nu_y = \int \frac{\left|\Phi(\nu_x, \nu_y)\right|^2}{\Delta\nu_x \Delta\nu_y} d\nu_y \qquad (1)$$

where PSD(ν_x) is the 1-D PSD, PSD(ν_x,ν_y) is the 2-D PSD, $\Phi(\nu_x,\nu_y)$ is the discrete fourier transform, $\Delta\nu_x$ and $\Delta\nu_y$ are the frequency steps, PSD(ν_x) is the 1-D PSD, and, and x,y can be rotated to any directions of interest. Since the measurement is taken over a finite area with a camera having a finite resolution, data valid regions of the PSD data exist between the vertical lines on the plot. The high frequency valid data limit is defined as half of the maximum frequency which can be displayed by the pixels of the camera (i.e. a full wave is five pixels). The low frequency data valid line is defined as six times the lowest frequency which can be displayed by the phase map, a half wave over the full aperture. The lowest frequencies are also not valid since the removal of focus and tilt from the phase data changes the value of the PSD for these frequencies. The straight line through the data corresponds to a fractal model[5] given by Eq. 2, where α = 1nm^2 mm and β = 1.55 (this value established by the actual measurement of many high quality optics) according to the specifications defined by the desired diffraction limited beam at the output of the Mercury laser:

$$F(\nu) = \alpha\nu^{-\beta} \tag{2}$$

where $F(\nu)$ is the specification function, ν is the spatial frequency, and α and β are constants. The Mercury specifications for a transmitted wavefront are approximately 5 times diffraction limited for the long axis of the 5-cm x 3-cm beam. The core and any other defective parts of a crystal can be removed by cutting the crystals and bonding the defect-free pieces together as shown in Fig. 3. Onyx Optics, Inc. in Dublin, CA, have made all of the crystal bonds to date with great success.

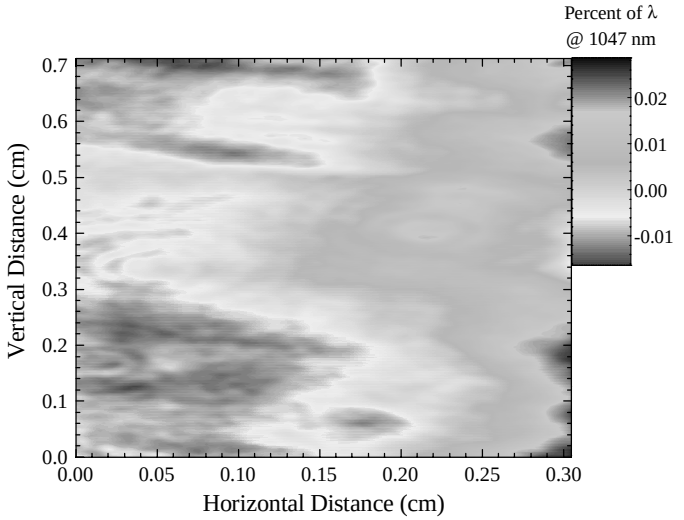

Fig. 1 Phase map of Yb:S-FAP crystal 6.54 mm thick

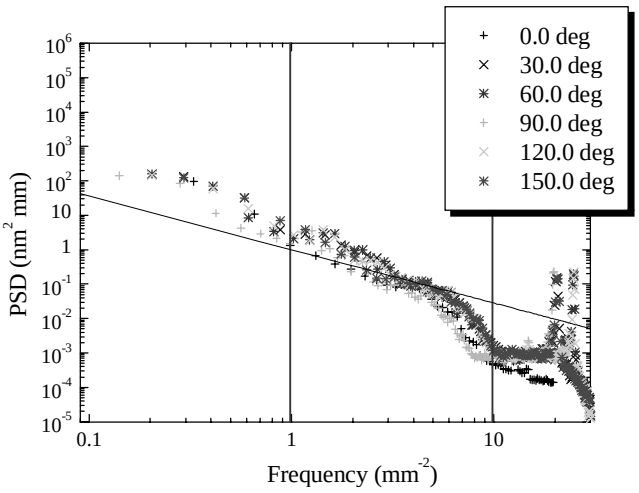

Fig. 2. Power Spectral Density (PSD) plot of Yb:S-FAP crystal 6.54 mm thick

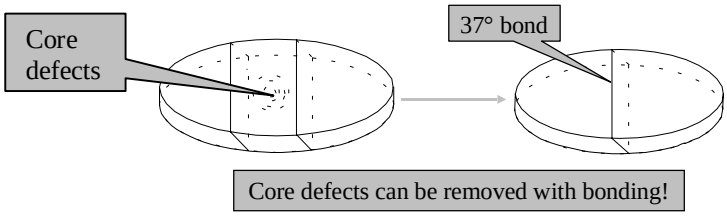

Fig. 3 Cartoon showing how bonding can be used for defect removal

The bonds are invisible to the naked eye and have a negligible negative impact on the phase maps, while allowing vast improvement of the overall transmitted phase of the crystal, since the best parts of a boule can be bonded together. Fig 4 shows the phase map of a typical bonded S-FAP crystal, while Fig. 5 compares the 1-D PSD of the unbonded part of the crystal with the 1-D PSD of the whole crystal including the bond. Clearly, bonding has almost no discerable impact on the 1-D PSD and therefore the diffraction limited beam quality of the Mercury output beam.

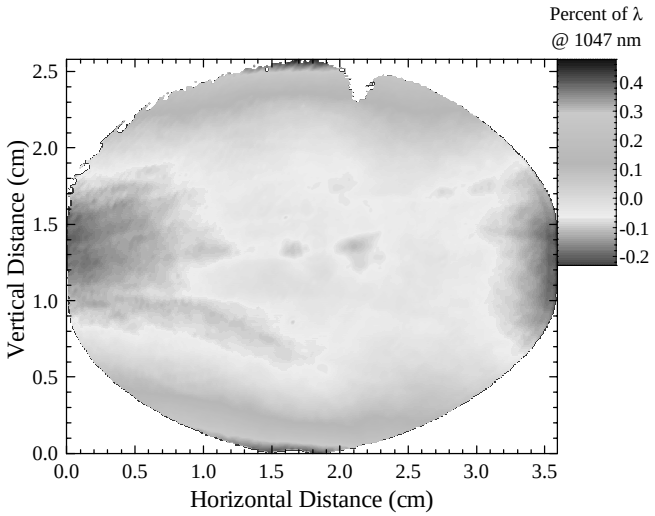

Fig. 4. Phase map of bonded S-FAP crystal

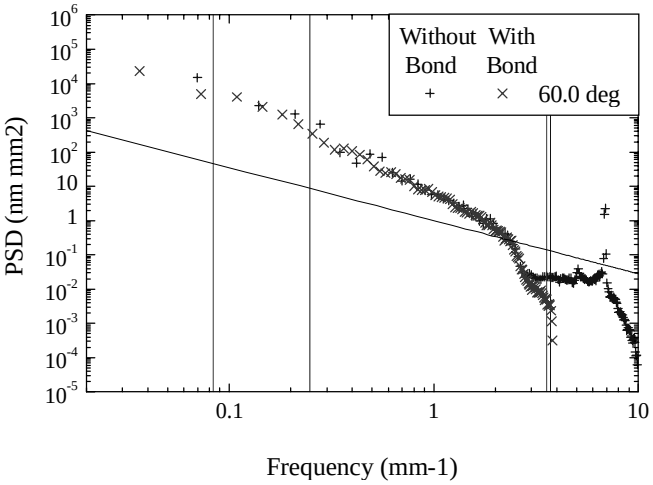

Fig. 5. 1-D PSD comparing the crystal phase map in Fig. 3 before and after bonding.

Gain Saturation

Measurement of gain saturation in S-FAP utilizes the generation of a high fluence pulsed source, shown below in Fig. 6 on the right hand side. A single stage Nd:YLF Master Oscillator Power Amplifier (MOPA) system is driven by a Q-switched Nd:YLF head (Spectra Physics Model 7960-L4-E) tuned for 1047 nm emission (coincident with the Yb:S-FAP emission peak). The amplifier is a flash lamp pumped Nd:YLF rod (0.25" x 3.0") mounted in Kigre pump chambers (FC-253-KK). The maximum energy output of the amplifier is approximately 40 mJ at 1047 nm, with a temporal pulsewidth of 8.1 ns Full-Width at Half Maximum (FWHM). The spatial profile of the output of the MOPA system was measured using a Cohu CCD camera (Model#4800) and a Coherent Beamview Analysis system to be an elliptical gaussian beam with $1/e^2$ widths of 760 and 780 microns at the Yb:S-FAP crystal location.

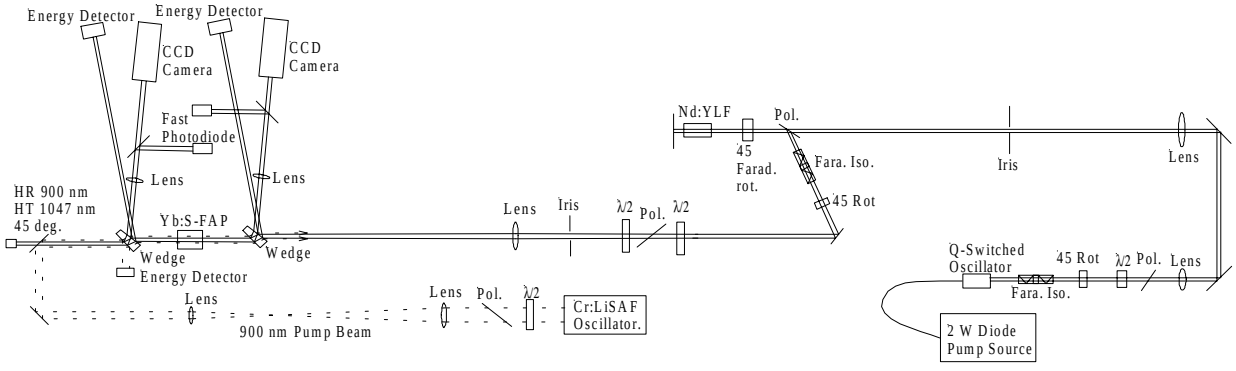

Fig. 6. Saturated Gain Experiment

Gain saturation studies were conducted using the experimental setup shown in the left-hand side of Fig. 6. The S-FAP is pumped by a flashlamp pumped Cr:LiSAF laser tuned to the 900 nm S-FAP absorption peak, with a maximum energy of 0.6 J, a temporal pulsewidth of 162 μs FWHM, and a spatial profile that was roughly flat topped with a $1/e^2$ diameter of 2 mm. Energy measurements were made using Molectron detectors for probe light (model J-9) and pump light (model J-25), while temporal measurements were made using Electro-Optics Technology photodetectors (model ET2000). Wedges at both the input and output ends of the crystal allowed simultaneous measurement of pump input, probe input, and probe output energy, as well as probe temporal and spatial profiles. The S-FAP sample is 1 atomic percent (at. %) ytterbium doped and approximately 3 cm long. The timing of the probe pulse was set to occur near the end of the pump pulse when the gain in the crystal was maximized. For these experiments, the gain was measured both as a function of pump fluence and as a function of extraction energy (recalling that the gaussian spatial profile of the probe beam represents a continuum of different fluences and must be treated numerically). Gain values at the output energy detector were measured relative to a null pump shot so that all passive losses (Fresnel reflections, scatter, and ytterbium absorption at the probe wavelength) are normalized out of the experiment.

A simulation code was written in C++ that modeled the transient energy level populations for a 2-level laser model, including the thermal population in the lower level of the ytterbium quasi-three level system, which is approximately 5%. The sample was divided into discrete spatial slices and the pump pulse into temporal intervals, and these temporal intervals were propagated consecutively through the spatial slices[6]. The transient small signal gain can then be calculated using Eq. 3:

$$G_0 = \exp\left[N_{ex}\sigma_{em}(\upsilon)\ell - N_{gr}\sigma_{abs}(\upsilon)\ell\right] \tag{3}$$

where N_{ex} and N_{gnd} are the excited and ground state populations respectively, σ_{em} and σ_{abs} are the emission and absorption cross sections of Yb:S-FAP at the laser frequency, and ℓ is the crystal length. Since the experiments measured peak gain, the calculation was stopped when excited state population and thus the small signal gain were maximized. The gaussian spatial profile of the probe pulse presents a small problem, since the extraction part of the calculation requires a fluence value. By breaking the gaussian into a set of concentric shells of constant amplitude, the profile can be approximated to arbitrary accuracy. Each of these shells has a constant fluence, and can therefore be propagated through the code. The shells are then reassembled at the output of the code to give the total output energy and gain for a given input energy. Since the extraction pulses are short compared to the emission lifetime, a Franz-Nodvik approach was used employing Eq. 4 to model the extraction.

$$G = \frac{F_{out}}{F_{in}} = \frac{F_{sat}}{F_{in}} \ln\left[(1 + G_0\left(\exp\left(\frac{F_{in}}{F_{sat}}\right) - 1\right)\right] \tag{4}$$

where G is the saturated gain, F_{out} is the output fluence, F_{sat} is the saturation fluence, G_0 is the small signal gain, and F_{in} is the input fluence. The gain was normalized to one at zero pump fluence to match experimental conditions (i.e. presence of ground state absorption and losses), and the results of the experiment and the modeling are given in Fig. 7, with the data points represented as large gray-scale spheres and the model fit points as a mesh. The fit value for the gain cross section is 6.2×10^{-20} cm^2 which corresponds to a saturation fluence of approximately 3.3 J/cm^2. Although an inhomogeneous model was initially employed in anticipation of an inhomogeneous extraction, the data fit to a single homogeneous extraction (or $k[g_u, g_L, F_{out}, \tau] = 1$) cross section as shown in Fig. 8.

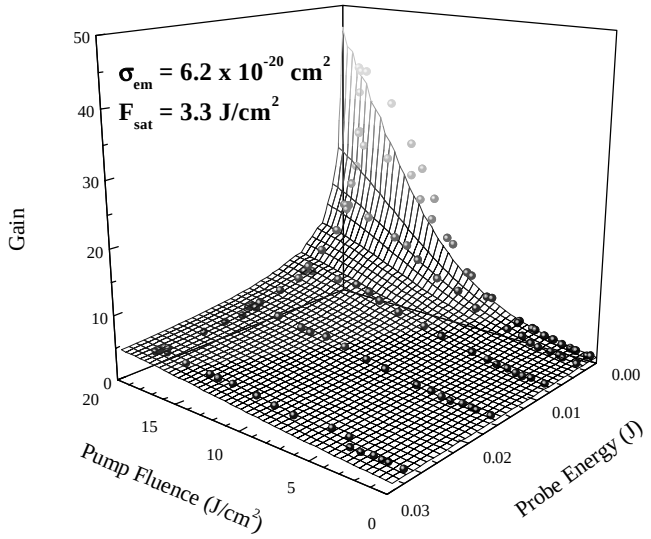

Fig. 7. Gain versus pump fluence and probe energy

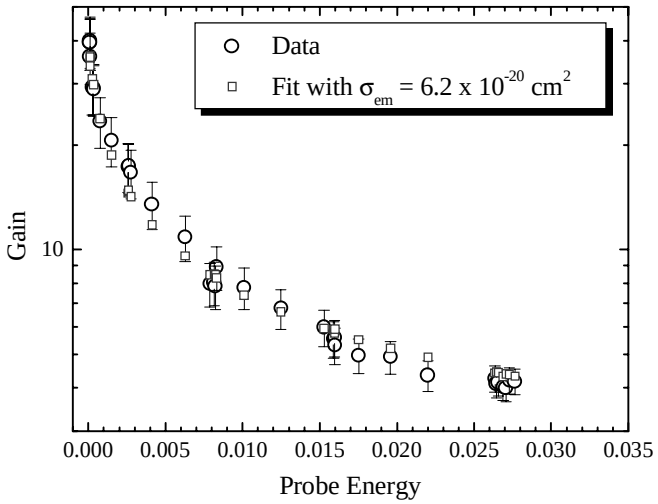

Fig. 8. Gain versus probe energy at peak pump fluence = 18 J/cm^2 with error analysis.

Summary

In conclusion, new methods have been developed to reduce the defects occuring in CZ grown Yb:S-FAP crystals. The optical homogeneity of the S-FAP crystals was measured and compared to PSD specifications for the Mercury project. The results indicate that recently grown crystals are close to the Mercury specifications for a 5x diffraction limited beam. Using a code which has been developed to handle transient pump, transient probe, and a spatially-dependent probe pulse, the saturated gain characteristics of ytterbium doped S-FAP have been quantified experimentally and modeled. The results indicate that homogeneous extraction is possible at the 1047 nm gain peak with a saturation fluence of 3.3 J/cm^2.

Acknowledgements

Special thanks to William Eickelberg for help in making the interferometry measurements, and Ralph Hutchinson of Scientific Materials for sharing his insights regarding SrF_2 evaporation. We would also like to acknowledge John Tassano for his tireless work on the CZ growth stations. This work was performed under the auspices of the U.S. Department of Energy by Lawrence Livermore National Laboratory under contract No. W-7405-Eng-48.

References

1. C.D. Marshall, L.K. Smith, R.J. Beach, M.A. Emanuel, K.I. Schaffers, J. Skidmore, S.A. Payne, and B.H.T. Chai, "Diode-pumped ytterbium-doped $Sr_5(PO_4)_3F$ laser performance," *IEEE J. Quan. Elec.* 32, 650-656 (1996).
2. C.D. Marshall, S.A. Payne, L.K. Smith, H.T. Powell, W.F. Krupke, and B.H.T. Chai, "1.047-μm $Yb:Sr_5(PO_4)_3F$ energy storage optical amplifier," *IEEE J. Sel. Top. Quan. Elec.* 1, 67-77 (1995).
3. S.M. Yarema, and D. Milam, "Gain saturation in phosphate laser glasses," *IEEE J. Quan. Elec.* 18, 1155-1163 (1982).

4. K.I. Schaffers, J.B. Tassano, S.A. Payne, R.L. Hutcheson, R.L. Equall, and B.H.T. Chai, “Crystal growth of Yb:$Sr_5(PO_4)_3F$ for 1.047-μm laser operation,” *OSA Trends in Optics and Photonics, Advanced Solid-State Lasers*, 19, 437-441 (1998).
5. E.L. Church, “Fractal surface finish,” *Applied Optics*, 27, 1518-1526 (1988).
6. A.J. Bayramian, C.D. Marshall, K.I. Schaffers, and S.A. Payne, "Characterization of Yb^{3+}:$Sr_{5-x}Ba_x(PO_4)_3F$ crystals for diode-pumped lasers," Submitted *IEEE J Quan. Elec.*, (1998).